Aging-related changes in blood-brain barrier integrity and the effect of dietary fat.

Takechi R[1,2], Pallebage-Gamarallage MM[1,2], Lam V[1,2], Giles C[1,2] and Mamo JC[1,2]

[1]Curtin Health Innovation Research Institute, School of Public Health, Faculty of Health Science, Curtin University, WA, Australia
[2]Centre for Metabolic Fitness, Australian Technology Network, WA, Australia

Corresponding author: Prof. John Mamo, email: J.Mamo@curtin.edu.au, Phone: +61 8 9266 7232, Fax: +61 8 9266 2958, Postal address: GPO Box 1987, Perth, WA, 6845 Australia.

Background: Disturbances in blood-brain barrier (BBB) integrity contribute to onset and progression of neurodegenerative diseases including Alzheimer's disease (AD) and vascular dementia (VaD). Aging is positively associated with AD and VaD risk, but this may reflect co-morbidities or the effects of other chronic modulators of vascular function such as diet. To explore putative synergistic effects of aging with diet, in this study genetically unmanipulated mice were maintained on diets enriched in saturated fatty acids (SFA) or cholesterol and compared to mice provided with low-fat feed formula.

Methods: The functional integrity of the BBB was assessed following 3, 6 and 12months of dietary intervention commenced at 6 weeks of age, by determining the brain parenchymal extravasation of immunoglobulin-G (IgG).

Results: Mice maintained on the SFA or cholesterol enriched diet showed significant parenchymal IgG abundance following 3 months of feeding, concomitant with diminished expression of the tight junction protein occludin. Low-fat control mice had essentially no evidence of BBB disturbances. Six months of SFA feeding exacerbated the difference in IgG abundance compared to the low-fat fed mice. At 12 months of feeding, the control low-fat fed mice also had significant parenchymal IgG that was comparable to mice fed the SFA or cholesterol enriched diets for 3 months. However, there may have been an adaptation to the fat enriched diets because SFA and cholesterol did not exacerbate IgG parenchymal accumulation beyond six months of feeding.

Conclusion: Collectively, the study suggests that diets enriched in SFA or cholesterol accelerate the onset of BBB dysfunction that otherwise occurs with aging.

Keywords: aging, blood-brain barrier, cholesterol, neurodegenerative disorder, neuroinflammation, saturated fatty acid

1.0 Introduction

Blood-brain barrier (BBB) is a fully differentiated neurovascular endothelial structure in the brain. The BBB consists of the tight junctions of vascular endothelial cells overlayed on basement membranes and has a critical function excluding plasma-derived neuro-toxic and inflammatory agents [1]. Several lines of evidence suggest that chronic disturbances of BBB function heighten neuronal inflammation and are likely to contribute to progression of neurodegenerative disorders such as Alzheimer's disease (AD), vascular dementia (VaD), multiple sclerosis or Parkinson's disease [2,3]. Indeed in all these disorders, brain parenchymal extravasation of plasma proteins, perivascular gliosis and lacunar lesions are commonly reported, observations consistent with breakdown of the BBB [4-6].

Risk for several neurodegenerative disorders including AD and VaD are influenced by lifestyle choices including nutrition [7-9]. Population and clinical studies show a positive association of AD with dietary cholesterol and saturated fatty acids (SFA) [10,11], whereas both mono- and poly-unsaturated fatty acids (MUFA and PUFA respectively) appear to confer protection for risk of AD [12-14]. One mechanism for the association between dietary fats and AD may be via modulation of BBB function. In genetically unmanipulated mice, chronic ingestion of diets enriched with SFA or cholesterol, but not in MUFA or PUFA, attenuated the expression of endothelial tight junction proteins and resulted in parenchymal extravasation of plasma proteins including circulating amyloid-beta [15]. Ghribi et al made similar findings in wild-type rabbits maintained on cholesterol-supplemented diets and showed amyloid-like plaque pathology [16] and in amyloid transgenic mice, SFA/cholesterol enriched diets were shown to significantly exacerbate cerebral amyloidosis [17,18].

Age is positively associated with the prevalence of dementia [19]. In the United States of America, 20% of the population older than 65 years and 50% of the population older than 80 years have probable AD or VaD. Several mechanisms could notionally explain the 'age-induced' increased risk for dementia phenomenon, but these commonly describe chronically

heightened states of systemic inflammation induced by co-morbidities such as diabetes, cardiovascular disease and stroke, or because of lifestyle behaviour such as poor nutrition and being sedentary [3,8]. In rodent models, otherwise healthy aged mice and rats maintained on diets containing just 4% of energy as fat and with little or no SFA/cholesterol nonetheless feature BBB abnormalities in comparison to younger aged animals [3,20,21]. The latter suggests independent but possibly synergistic effects with other co-morbidities and vascular stressors. Accordingly, this study was designed to investigate BBB function in wild-type mice that were maintained on either a low-SFA and cholesterol-free diet, or a diet enriched with either SFA, or with cholesterol for 3, 6 and 12 months.

2.0 Materials and methods

2.1 Animals and dietary treatments

Six-week old, female C57BL/6J mice were purchased from Animal Resources Centre (Murdoch, WA, Australia). Mice were held in the accredited animal holding facility (Building 300, Curtin University) with 12 h light/dark cycle and controlled air temperature and pressure. Mice had ad libitum access to the feed and water.

Groups of 24 mice were randomly allocated to each dietary treatment group. A semi-synthetic mice chow diet was provided by Specialty Feeds, (Glenn Forrest, WA, Australia). Control low-fat diet was the standard rodent chow; AIN93M containing 4% (w/w) of dietary fats as polyunsaturated oil and no cholesterol (see table 1 for detail). The cholesterol diet was produced by providing 1% (w/w) cholesterol into the AIN93M control chow. An enriched SFA diet was prepared by adding 20% (w/w) of SFA derived from cocoa butter. Digestible energy from the cocoa butter in SFA diet was 40% and the main fatty acids in the diet were palmitic (16:0, 5%), stearic (18:0, 7%) and oleic acid (18:1n-9, 6%) (Table 1). Eight mice from each group were sacrificed at 3, 6 and 12 months after the commencement of dietary treatment, and the brain and plasma samples were collected for the analysis as described previously [15].

All experimental procedures in this study were approved by a National Health and Medical Research Council of Australia accredited Animal Ethics Committee (Curtin University approval no: R08-10).

2.2 Quantitative immunofluorescent microscopy of cerebral IgG extravasation

The integrity of the BBB was determined by the detection of cerebral perivascular extravasation of plasma protein, IgG. This is a widely used and established method [22,23] and in this study we used published quantitative 3-D immuno-microscopy methods described previously [8,9,15,24-26] with minor modifications. The right hemisphere of the brain was carefully isolated and washed in ice-cold PBS. The brain tissues were immersion-fixed in 4% paraformaldehyde for 24 h and cryoprotected in 20% sucrose for 3 days. The tissues were then frozen in isopentane/dry ice and stored at -80°C. Brain cryosections of 20μm were prepared on polysine coated microscope slides and the unspecific binding sites were blocked with 10% goat serum in PBS for 30 min. Goat anti-mouse IgG conjugated with Alexa488 fluorochrome (Invitrogen, US) was applied to the sections at a concentration of 1:50 in PBS, and incubated at 4 °C for 20 h. After a thorough wash of the sections with PBS, DAPI counter staining (Invitrogen) was done for nuclei detection, and the sections were mounted with anti-fade mounting medium.

The immunofluorescent micrographs were taken in 3-D with AxioVert 200M (Carl-Zeiss, Germany) coupled with mRM digital camera and ApoTome optical sectioning system. Each 3-D image was captured at a magnification of x200 (Plan-Neofluar 20x objective lens) and consisted of at least twelve 2-D Z-stack images with 1.225 μm axial distance optimized by Nyquist theory. For each cortex and hippocampal formation regions 5-12 three-dimensional images were randomly taken from each brain section, and all the 3-D images were used for the following quantitative analysis. Fluorescent voxel intensity of the IgG perivascular

extravasation was calculated with Volocity 3-D image analysis software (PerkinElmer, UK) and expressed as per volume unit.

2.3 Immunofluorescent quantitative analysis of the cerebrovascular tight junction protein, occludin-1

The abundance of cerebrovascular tight junction, occludin-1, relative to the endothelium was quantitatively determined in the cortex and hippocampus using three-dimensional double immunofluorescent microscopy as described previously [15,24]. Briefly, the brain cryosections (20 μm thick) were fixed with acetone at -20 °C for 3 min and heat-mediated antigen retrieval was conducted by incubating the sections in 60 °C water for 2 h. Endogenous biotin was blocked with avidin in egg white and biotin in skimmed milk. In order to avoid the cross-reaction of the two polyclonal antibodies, the concentration of the first antibody was diluted so that it was undetectable with conventional secondary antibody detection, but detectable after the biotin-avidin signal amplification. The sections were incubated with rabbit anti-mouse occludin-1 (1:200, Invitrogen) for 20 h at 4 °C after blocking of unspecific biding sites with 10% goat serum. The sections were then incubated with anti-rabbit IgG conjugated with biotin (1:200, DAKO) for 2 h at 20 °C. Rabbit anti-von-Willebrand factor (1:200, Abcam) was applied to the sections for 2 h at 20 °C. Finally the sections were incubated with a mixture of avidin conjugated with Alexa546 and anti-rabbit IgG conjugated with Alexa488. The nuclei were counterstained with DAPI. The colocalization of occludin-1 and vWF was determined, and the optical pixel intensity of the occludin-1 in the colocalized area was calculated with AxioVision imaging software. The total vWF expression was also determined by calculating the voxel intensity with Volocity. The cerebrovascular expression of occludin-1 was expressed as relative to the total vWF expression.

2.4 Immunofluorescent analysis of cerebral GFAP and its colocalization with perivascular IgG extravasation

Similar to cerebral IgG immuno-microscopy, the cortex and hippocampus expression of GFAP was determined as a surrogate marker for astrocyte activation by utilizing quantitative immunofluorescent microscopy. The brain cryosections were blocked with 10% goat serum and incubated with rabbit anti-mouse GFAP (1:500, Abcam, UK) for 20 h at 4 °C. Goat anti-rabbit IgG with Alexa546 was then added to the section for 1 h, and the sections were counter stained with DAPI.

The colocalization of activated GFAP with the cerebral perivascular IgG leakage was also determined with double immunofluorescent staining. A mixture of goat anti-mouse IgG Alexa488 and rabbit anti-mouse GFAP was applied to the sections and incubated for 20 h at 4 ^{o}C. After a thorough wash, anti-rabbit IgG Alexa546 was added to the sections and incubated for 1 h. The colocalization of 2 proteins was analyzed by Volocity.

2.5 Determination of plasma S100B

S100B is a calcium binding protein predominantly produced by astrocytes and abundant in cerebrospinal fluid but not in peripheral tissue or plasma [27]. The CSF and/or plasma S100B is elevated in a number of neurodegenerative diseases including stroke and schizophrenia [28-30]. Therefore the plasma concentration of S100B is often used as a marker of BBB integrity and cerebrovascular inflammation [27,31,32]. Plasma S100B was measured by ELISA kit (CosmoBio, Japan) as per the instructions provided by the manufacturer. Briefly, 20 µl of plasma samples, or of the S100B standards (0, 98, 197, 394, 1575, 3150 and 6300 pg/ml) were incubated overnight at 4 ^{o}C in 96-well microplates coated with the primary antibody. Thereafter, plates were incubated with conjugated secondary antibody for 2 hours, followed by 2 hours incubation with streptavidin-HRP. Finally samples were incubated with substrate

solution for 20 min and the reaction was terminated with stopping solution. The optical absorbance was measured at 490 nm.

2.6 Plasma lipid assays

Plasma total cholesterol and triglycerides were determined with colorimetric assays (Randox, UK) according to the manufacturer's instruction with minor modifications. Briefly, 2 μL of sample plasma or standard solution was added to 96-well microplate, and 200 μL of assay reagent was added. Samples were incubated for 5 min at 37 ^{o}C and the optical absorbance was measured at 500nm. For cholesterol assay, standard was plotted at 0, 1.25, 2.5 and 5.0 mmol/L. For triglycerides assay, standard was plotted at 0, 1.1 and 2.19 mmol/L.

2.7 Statistics

For the quantitative immuno-microscopy a minimum of 60 two-dimensional images were taken from each mouse and in total more than 480 images per group. For IgG extravasation, plasma S100B and cerebral GFAP, the cumulative effects through the entire experimental period were estimated by analyzing the area under the curve (AUC). The calculation of standard deviations for AUC was conducted according to the method of Bailer [33]. One-way ANOVA followed by post hoc tests was used to determine the statistical significance (p<0.05, SPSS). For plasma lipid assays, the Pearson's correlation coefficient of plasma lipid level and BBB disruption (Voxel intensity of IgG extravasation) was analyzed in each mouse on GraphPad Prism.

3.0 Results

The effect of aging and potential synergistic effects with diets enriched in either SFA or cholesterol on parenchymal extravasation of IgG is demonstrated in figure 1 and quantitatively compared in figure 2 for different durations of feeding. After 3 months of

dietary intervention, there was limited IgG abundance within brain parenchyme in mice maintained on the LF-control diet. However, in LF-fed mice there was a four- and nine-fold increase in plasma derived IgG after 6 and 12 months of dietary intervention respectively (Fig 2A).

We confirm that mice maintained on a diet supplemented with cholesterol, or enriched with SFA for 3 months had substantially greater parenchymal IgG abundance than control mice on the LF-diet (Fig 2A). However, interactive effects with age became evident particularly in mice maintained on the SFA enriched diet. Expressed as the cumulative index of IgG abundance (ie area under the curve between 3 and 12 months of feeding; CIG_{AUC}), mice maintained on SFA had a 3-fold greater rate of IgG accumulation than the LF-control group (Fig 2B). Cholesterol supplemented mice like the SFA fed mice had an earlier onset of parenchymal accumulation of IgG compared to LF-controls with significant divergence between the two groups at 3 months. However, after 12 months of dietary intervention, the two groups showed similar levels of parenchymal IgG abundance. Indeed, there was no difference in CIG_{AUC} up to 12 months of feeding for the cholesterol-supplemented versus LF-control mice (Fig 2B).

Considering brain-to-blood leakage of S100B mirrored the significant differential effects of aging and dietary SFA/cholesterol on BBB integrity. Mice maintained on the LF-diet showed a remarkable increase in plasma S100B after 12 months of dietary intervention compared to 3 months (Fig 3A). Similarly, the SFA or dietary cholesterol supplemented mice had marked elevations in plasma S100B at 3 months of feeding. The cumulative plasma index of S100B ($CIS100B_{AUC}$) was significantly increased in the SFA fed mice (Fig 3B), but there was no difference between cholesterol fed mice and LF-controls. Concomitant with increased plasma S100B and parenchymal abundance of IgG, was a significant reduction in the endothelium abundance of the tight junction occludin-1 (Fig 4).

To explore if disturbances in BBB function induced by aging and accelerated onset by dietary SFA or cholesterol was associated with cerebrovascular inflammation, determining the

abundance of GFAP and its putative colocalization with parenchymal IgG accumulation assessed the activation of cerebral astroglial cells. Figure 5 shows the exaggerated abundance of GFAP and significant co-localisation with IgG in LF-control mice after 12 months of dietary intervention. The GFAP/IgG association was also evident in the SFA fed mice and cholesterol fed mice (not illustrated). Consistently, the Pearson's correlation coefficient analysis showed a significant correlation (p<0.0001) between the cerebral GFAP expression and IgG association in all groups (Fig 6C). The expression of GFAP in the cortex was greater in SFA and cholesterol supplemented mice after 3 months of dietary intervention but there was no significant difference between the groups at 12 months (Fig 6A). An accelerated inflammatory onset associated with SFA feeding is suggested by the cumulative index of cortex GFAP ($CIGFAP_{AUC}$) which was greater in the SFA fed mice compared to LF control.

Plasma lipids were determined to explore if there was an association with the parenchymal appearance of IgG in aged and SFA/cholesterol supplemented mice. The diets given to mice were well tolerated and similar rates of weight gain were observed in all groups of mice (data not shown). The SFA fed mice were hypertriglyceridemic at 3 months of feeding compared to LF-control mice, but there was no difference by 12 months of intervention between the groups of mice (Fig 7C). Whereas mice maintained on cholesterol became hypercholesterolemic and the divergence compared to the LF-control group increased with age (Fig 7A). Correlation analysis found no association of plasma triglyceride concentration and cerebral IgG extravasation (Fig 7D). In contrast, there was a modest but nonetheless statistically significant association between plasma cholesterol and parenchymal IgG (Fig 7B).

4.0 Discussion

An accumulating body of evidence suggests that the dysfunction of BBB followed by blood-to-brain leakage of plasma neuro-inflammatory substances may be important to the onset and progression of neurodegenerative disorders including AD and VaD. Some studies suggest that

the disruption of BBB occurs with normal aging, however this hypothesis may be confounded because of co-morbidities that develop with age, or because of persistent poor lifestyle choices including dietary behaviour. To explore the concept of an age-induced effect on BBB function and synergistic effects with dietary fats, in this study, a wild-type mouse model was used to examine whether BBB disruption develops in aging mice maintained on a low-fat and cholesterol free diet and whether this is influenced by diets enriched in SFA or cholesterol.

The blood-to-brain leakage of plasma protein, IgG (150 kDa), is a commonly used approach to assess BBB integrity and function [16,22,23]. In this study we used an established highly sensitive immunofluorescent microscopy procedure to quantitatively assess the parenchymal abundance of IgG [15,24]. In addition, colocalisation analysis with specific markers of cerebrovascular inflammation (GFAP) were determined in three-dimensions.

Consistent with previous studies [15], we confirm the significant parenchymal abundance of IgG in mice maintained on SFA, or a cholesterol-rich diet for 3 months. However, there was no evidence that this occurred in mice maintained on a low-fat and cholesterol-free diet for 3 months. Accumulation of parenchymal IgG occurred concomitant with a significant reduction in the endothelial tight junction protein occludin-1 consistent with disturbed BBB function. We extend on those findings and now demonstrate that parenchymal extravasation of IgG progressively increases in aging mice maintained in what is considered a balanced LF-diet. Indeed, there was a strong association of IgG extravasation and age, with substantially greater IgG after 12 months of dietary intervention, compared to 6 months. Confirmation of an age-induced effect was also supported by findings of the plasma concentration of the neuronal peptide S100B. Mice maintained on the LF diet had significantly greater plasma S100B after 12 months of dietary intervention > 6 months compared to 3 months. Collectively, the data suggests that BBB function becomes progressively compromised with age, resulting in bidirectional and probably non-specific trafficking of proteins that are normally otherwise excluded. Given that the average life span of genetically unmanipulated laboratory mice is 18

to 20 months, the findings suggest that the phenomenon of plasma derived protein extravasation commences at approximately 'middle-age'.

Concomitant with parenchymal IgG extravasation in LF-control mice was evidence of cerebrovascular-specific inflammation equivocally demonstrated by increased expression of GFAP after 6 and 12 months of dietary intervention. Moreover, there was significant colocalisation of glial cell activation (indicated by GFAP) with IgG parenchymal penetration, consistent with a causal effect.

Up to 6-months of dietary intervention, the data indicates that there may have been synergistic effect of SFA with age, because divergence in the rate of IgG extravasation was observed between the two groups of mice (ie: difference between two groups continued to increase between 3 and 6 months of dietary intervention). However, beyond 6 months, SFA feeding did not appear to exacerbate BBB dysfunction compared to the effects of aging alone. The earlier onset and accelerated-induction response because of SFA feeding is supported by the finding of a substantially greater CIG_{AUC} in the SFA group compared to LF-aged mice. However, we cannot determine from this study, whether introduction of SFA in perhaps already aged mice with established BBB dysfunction will have an additive effect on deterioration.

Mice maintained on a diet containing an additional 1% of cholesterol by weight like the SFA-fed mice had accelerated onset of IgG accumulation within brain parenchyme compared to LF-fed mice. However, the differential effect induced by dietary cholesterol was no longer evident after 6 or 12 months of intervention. Following 6 months of feeding, the IgG extravasation was not significantly different to the LF-control group and neither was there any difference in the CIG_{AUC} or the $CIS100B_{AUC}$.

Collectively, given that neither dietary SFA nor cholesterol continues to exacerbate parenchymal extravasation of IgG beyond 6 months of intervention suggests either an adaptation response to the fat enriched diets, or perhaps a sub-maximal effect. The former is

more likely given the persistent difference between the 12 months SFA-feeding, versus either the cholesterol-fed or LF-control groups of mice.

Several mechanisms could explain the accelerated onset phenomenon observed in SFA and cholesterol supplemented mice, however the reason for IgG extravasation in LF-control mice at older age is less obvious. Lipotoxicity is a term used for a process that leads to an end-organ damage caused by excessive cellular lipid overload. Morgan suggests that the underlying toxicity of SFA is a consequence of disturbances in protein processing and endoplasmic reticulum (ER) dysfunction, for example apoptotic induction [34]. One relevant example was a study by Patil et al. who found that dietary palmitic acid induced region-specific cerebral damage because of higher fatty acid-metabolizing capacity of cortical astroglia [35]. Conversely, cell culture studies suggest that incubation with longer chain unsaturates has an antagonistic effect on stress pathways [36]. Similarly Yao and colleagues suggest that excess cholesterol causes ER and mitochondrial stress that can lead to apoptosis [37]. Mitochondrial activity or lysosomal processing can result in the production of oxidized lipids including cholesterol. A number of studies support the contention that oxidized lipids compromise tissue integrity and exacerbate inflammatory pathways [38,39]. However, if mitochondrial and ER stress are central to the effects of SFA and cholesterol, it is unclear how the effects would become mitigated with increased duration of feeding.

The data in this study showed a significant increase in plasma cholesterol in cholesterol fed mice, but there was only a weak positive association with BBB dysfunction. The SFA supplemented mice showed no changes in plasma cholesterol and triglyceride. Hence, we cannot completely rule out an effect of dyslipidemia.

Alternative explanations for BBB dysfunction with aging that is independent of co-morbidities or other obvious lifestyle related are relatively few. Repetitive hypoxic episodes were proposed to compromise capillary integrity either directly, or because of diminished VEGF mediated angiogenesis following hypoxic episodes (which tend to increase with age) [40-44].

Alternatively, what we ordinarily consider to be complete, balanced or otherwise healthy diets may in a chronic context be subtly inadequate or deficient. Another explanation is that transient episodes of inflammation in response to infection or injury, transient metabolic disturbances, or acute ingestion of pro-inflammatory compounds may provide repeated insults that are physiologically important, but difficult to monitor [4]. In this study, mice were closely assessed for infection or disease utilizing sentinel mice maintained within the same facility, but we did not identify any periods of infection with micro-organisms. On the other hand, the diet was not altered for the duration of the study and so nutrient insufficiency, or other dietary pro-inflammatory components cannot be ruled out. Finally, only modest environmental enrichment was provided (limited to 'hide boxes'), which may have resulted in stress related effects.

In conclusion, this study for the first time quantitatively demonstrated a progressive decline in BBB function as a consequence of aging in genetically unmanipulated mice maintained on a low-fat and cholesterol free diet. Early introduction of diets enriched in SFA or cholesterol were found to accelerate the onset of BBB dysfunction that occurs with aging. Dietary SFA, but not cholesterol had a synergistic effect with aging on the degree of BBB dysfunction over the first six months of feeding, that persisted in mice after 12 months of dietary intervention. These data are informative in the context of risk for neurodegenerative disorders that feature cerebrovascular disturbances.

Acknowledgement

This project was supported by National Health and Medical Research Council (Australia) Project Grant. R.T. was supported by National Health and Medical Research Council Fellowship and Curtin Research Fellowship.

Disclosure statement

Authors declare no conflict of interests.

5.0 References

1 Abbott, NJ, Patabendige, AA, Dolman, DE, Yusof, SR and Begley, DJ: Structure and function of the blood-brain barrier. Neurobiol Dis 2010;37:13-25

2 Zlokovic, BV: The blood-brain barrier in health and chronic neurodegenerative disorders. Neuron 2008;57:178-201

3 Vasilevko, V, Passos, GF, Quiring, D, Head, E, Kim, RC, Fisher, M and Cribbs, DH: Aging and cerebrovascular dysfunction: contribution of hypertension, cerebral amyloid angiopathy, and immunotherapy. Ann N Y Acad Sci 2010;1207:58-70

4 Kalaria, RN: Vascular basis for brain degeneration: faltering controls and risk factors for dementia. Nutr Rev 2010;68 Suppl 2:S74-87

5 Dickstein, DL, Walsh, J, Brautigam, H, Stockton, SD, Jr., Gandy, S and Hof, PR: Role of vascular risk factors and vascular dysfunction in Alzheimer's disease. Mt Sinai J Med 2010;77:82-102

6 Miyakawa, T: Vascular pathology in Alzheimer's disease. Psychogeriatrics 2010;10:39-44

7 Luchsinger, JA and Mayeux, R: Dietary factors and Alzheimer's disease. Lancet Neurol 2004;3:579-87

8 Takechi, R, Galloway, S, Pallebage-Gamarallage, MM, Lam, V and Mamo, JC: Dietary fats, cerebrovasculature integrity and Alzheimer's disease risk. Prog Lipid Res 2010;49:159-70

9 Takechi, R, Galloway, S, Pallebage-Gamarallage, MM and Mamo, JC: Chylomicron amyloid-beta in the aetiology of Alzheimer's disease. Atheroscler Suppl 2008;9:19-25

10 Laitinen, MH, Ngandu, T, Rovio, S, Helkala, EL, Uusitalo, U, Viitanen, M, Nissinen, A, Tuomilehto, J, Soininen, H and Kivipelto, M: Fat intake at midlife and risk of dementia and Alzheimer's disease: a population-based study. Dement Geriatr Cogn Disord 2006;22:99-107

11 Oksman, M, Iivonen, H, Hogyes, E, Amtul, Z, Penke, B, Leenders, I, Broersen, L, Lutjohann, D, Hartmann, T and Tanila, H: Impact of different saturated fatty acid,

polyunsaturated fatty acid and cholesterol containing diets on beta-amyloid accumulation in APP/PS1 transgenic mice. Neurobiol Dis 2006;23:563-72

12 Hooijmans, CR, Van der Zee, CE, Dederen, PJ, Brouwer, KM, Reijmer, YD, van Groen, T, Broersen, LM, Lutjohann, D, Heerschap, A and Kiliaan, AJ: DHA and cholesterol containing diets influence Alzheimer-like pathology, cognition and cerebral vasculature in APPswe/PS1dE9 mice. Neurobiol Dis 2009;33:482-98

13 Scarmeas, N, Stern, Y, Mayeux, R, Manly, JJ, Schupf, N and Luchsinger, JA: Mediterranean diet and mild cognitive impairment. Arch Neurol 2009;66:216-25

14 Cunnane, SC, Plourde, M, Pifferi, F, Begin, M, Feart, C and Barberger-Gateau, P: Fish, docosahexaenoic acid and Alzheimer's disease. Prog Lipid Res 2009;48:239-56

15 Takechi, R, Galloway, S, Pallebage-Gamarallage, MM, Wellington, CL, Johnsen, RD, Dhaliwal, SS and Mamo, JC: Differential effects of dietary fatty acids on the cerebral distribution of plasma-derived apo B lipoproteins with amyloid-beta. Br J Nutr 2010;103:652-62

16 Ghribi, O, Golovko, MY, Larsen, B, Schrag, M and Murphy, EJ: Deposition of iron and beta-amyloid plaques is associated with cortical cellular damage in rabbits fed with long-term cholesterol-enriched diets. J Neurochem 2006;99:438-49

17 Refolo, LM, Malester, B, LaFrancois, J, Bryant-Thomas, T, Wang, R, Tint, GS, Sambamurti, K, Duff, K and Pappolla, MA: Hypercholesterolemia accelerates the Alzheimer's amyloid pathology in a transgenic mouse model. Neurobiol Dis 2000;7:321-31

18 Shie, FS, Jin, LW, Cook, DG, Leverenz, JB and LeBoeuf, RC: Diet-induced hypercholesterolemia enhances brain A beta accumulation in transgenic mice. Neuroreport 2002;13:455-9

19 2008 Alzheimer's disease facts and figures. Alzheimers Dement 2008;4:110-33

20 Mooradian, AD: Effect of aging on the blood-brain barrier. Neurobiol Aging 1988;9:31-9

21 Tripathy, D, Yin, X, Sanchez, A, Luo, J, Martinez, J and Grammas, P: Cerebrovascular expression of proteins related to inflammation, oxidative stress and neurotoxicity is altered with aging. J Neuroinflammation 2010;7:63

22 Beard, RS, Jr., Reynolds, JJ and Bearden, SE: Hyperhomocysteinemia increases permeability of the blood-brain barrier by NMDA receptor-dependent regulation of adherens and tight junctions. Blood 2011;118:2007-14

23 Elali, A, Doeppner, TR, Zechariah, A and Hermann, DM: Increased Blood-Brain Barrier Permeability and Brain Edema After Focal Cerebral Ischemia Induced by Hyperlipidemia: Role of Lipid Peroxidation and Calpain-1/2, Matrix Metalloproteinase-2/9, and RhoA Overactivation. Stroke 2011;

24 Takechi, R, Galloway, S, Pallebage-Gamarallage, MM, Johnsen, RD and Mamo, JC: Three-dimensional immunofluorescent double labelling using polyclonal antibodies derived from the same species: enterocytic colocalization of chylomicrons with Golgi apparatus. Histochem Cell Biol 2008;129:779-84

25 Van Broeck, B, Van Broeckhoven, C and Kumar-Singh, S: Current insights into molecular mechanisms of Alzheimer disease and their implications for therapeutic approaches. Neurodegener Dis 2007;4:349-65

26 Kumar-Singh, S, Pirici, D, McGowan, E, Serneels, S, Ceuterick, C, Hardy, J, Duff, K, Dickson, D and Van Broeckhoven, C: Dense-core plaques in Tg2576 and PSAPP mouse models of Alzheimer's disease are centered on vessel walls. Am J Pathol 2005;167:527-43

27 Marchi, N, Rasmussen, P, Kapural, M, Fazio, V, Kight, K, Mayberg, MR, Kanner, A, Ayumar, B, Albensi, B, Cavaglia, M and Janigro, D: Peripheral markers of brain damage and blood-brain barrier dysfunction. Restor Neurol Neurosci 2003;21:109-21

28 Herrmann, M and Ehrenreich, H: Brain derived proteins as markers of acute stroke: their relation to pathophysiology, outcome prediction and neuroprotective drug monitoring. Restor Neurol Neurosci 2003;21:177-90

29 Steiner, J, Bielau, H, Bernstein, HG, Bogerts, B and Wunderlich, MT: Increased cerebrospinal fluid and serum levels of S100B in first-onset schizophrenia are not related to a degenerative release of glial fibrillar acidic protein, myelin basic protein and neurone-specific enolase from glia or neurones. J Neurol Neurosurg Psychiatry 2006;77:1284-7

30 Rothermundt, M, Ohrmann, P, Abel, S, Siegmund, A, Pedersen, A, Ponath, G, Suslow, T, Peters, M, Kaestner, F, Heindel, W, Arolt, V and Pfleiderer, B: Glial cell activation in a subgroup of patients with schizophrenia indicated by increased S100B serum concentrations and elevated myo-inositol. Prog Neuropsychopharmacol Biol Psychiatry 2007;31:361-4

31 Kleindienst, A, Hesse, F, Bullock, MR and Buchfelder, M: The neurotrophic protein S100B: value as a marker of brain damage and possible therapeutic implications. Prog Brain Res 2007;161:317-25

32 Chaves, ML, Camozzato, AL, Ferreira, ED, Piazenski, I, Kochhann, R, Dall'Igna, O, Mazzini, GS, Souza, DO and Portela, LV: Serum levels of S100B and NSE proteins in Alzheimer's disease patients. J Neuroinflammation 2010;7:6

33 Bailer, AJ: Testing for the equality of area under the curves when using destructive measurement techniques. J Pharmacokinet Biopharm 1988;16:303-9

34 Morgan, NG: Fatty acids and beta-cell toxicity. Curr Opin Clin Nutr Metab Care 2009;12:117-22

35 Patil, S, Sheng, L, Masserang, A and Chan, C: Palmitic acid-treated astrocytes induce BACE1 upregulation and accumulation of C-terminal fragment of APP in primary cortical neurons. Neurosci Lett 2006;406:55-9

36 Diakogiannaki, E and Morgan, NG: Differential regulation of the ER stress response by long-chain fatty acids in the pancreatic beta-cell. Biochem Soc Trans 2008;36:959-62

37 Yao, PM and Tabas, I: Free cholesterol loading of macrophages is associated with widespread mitochondrial dysfunction and activation of the mitochondrial apoptosis pathway. J Biol Chem 2001;276:42468-76

38 Clare, K, Hardwick, SJ, Carpenter, KL, Weeratunge, N and Mitchinson, MJ: Toxicity of oxysterols to human monocyte-macrophages. Atherosclerosis 1995;118:67-75

39 Peng, SK, Tham, P, Taylor, CB and Mikkelson, B: Cytotoxicity of oxidation derivatives of cholesterol on cultured aortic smooth muscle cells and their effect on cholesterol biosynthesis. Am J Clin Nutr 1979;32:1033-42

40 Black, JE, Polinsky, M and Greenough, WT: Progressive failure of cerebral angiogenesis supporting neural plasticity in aging rats. Neurobiol Aging 1989;10:353-8

41 Rivard, A, Fabre, JE, Silver, M, Chen, D, Murohara, T, Kearney, M, Magner, M, Asahara, T and Isner, JM: Age-dependent impairment of angiogenesis. Circulation 1999;99:111-20

42 Chavez, JC and LaManna, JC: Hypoxia-inducible factor-1alpha accumulation in the rat brain in response to hypoxia and ischemia is attenuated during aging. Adv Exp Med Biol 2003;510:337-41

43 Rapino, C, Bianchi, G, Di Giulio, C, Centurione, L, Cacchio, M, Antonucci, A and Cataldi, A: HIF-1alpha cytoplasmic accumulation is associated with cell death in old rat cerebral cortex exposed to intermittent hypoxia. Aging Cell 2005;4:177-85

44 Rivard, A, Berthou-Soulie, L, Principe, N, Kearney, M, Curry, C, Branellec, D, Semenza, GL and Isner, JM: Age-dependent defect in vascular endothelial growth factor expression is associated with reduced hypoxia-inducible factor 1 activity. J Biol Chem 2000;275:29643-7

6.0 Figure Legends

Table 1. Detailed dietary composition of mouse chow. The table shows the detailed lipid composition in the diets used in this study. Control diet was AIN93M standard low-fat rodent chow containing no cholesterol and 4% unsaturated fats. The cholesterol diet contained 1% (w/w) of sterol. Saturated fat (SFA) diet contained 20% (w/w) saturated fats from cocoa butter.

Figure 1. 3-D immunofluorescent microscopy of cerebral IgG extravasation. The integrity of the BBB was assessed by the cerebral extravasation of plasma protein, IgG. The immunofluorescent micrographs show the distribution of IgG in the brain (green) of low-fat control, high-cholesterol or high-saturated fat (SFA) fed mice following 3 months and 12 months of dietary intervention. DAPI counterstaining was used to stain the nuclei (blue). The upper frames show the 2-D extended focus micrographs of 3-D images taken at a magnification of x200 (scale bar=100 μm). The lower frames are the magnified 3-D micrographs of the indicated area of the white rectangle in the 2-D images; with dimensions of 206 μm (X axis), 154 μm (Y axis) and 12.25 μm (Z axis).

Figure 2. 3-D semi-quantitative analysis of blood-brain barrier integrity. As a marker of blood-brain barrier dysfunction, cerebral IgG extravasation was quantitatively determined in 3-D in animals maintained on diets with low-fat control, saturated fat (SFA) enriched or cholesterol supplemented diets. **(A)** Voxel intensity of perivascular fluorescent IgG staining in the image was measured per volume unit. Data are shown as mean±SEM. Data significantly differ from control (Dietary effects) is indicated by * (n=8, $p<0.05$, one-way ANOVA), and significance within each group (Aging/Duration effects) is indicated by alphabetical letters (n=8, $p<0.05$, one-way ANOVA). **(B)** In addition, the total cumulative IgG extravasation during the entire dietary intervention period was estimated by calculating the area under the curve

(AUC±SD). Statistical significance is indicated with alphabetical letters (n=8, p<0.05, one-way ANOVA).

Figure 3. Plasma marker of blood-brain barrier integrity. (A) The plasma concentration of S100B was measured with ELISA kits as a surrogate marker for blood-brain barrier dysfunction in mice maintained on a cholesterol-free low-fat diet, or a diet enriched in saturated fat diet (SFA) or cholesterol. Data are shown as mean±SEM. Data significantly differ from control (Dietary effects) are indicated by * (n=8, p<0.05, one-way ANOVA), and significance within each group (Aging/Duration effects) is indicated by alphabetical letters (n=8, p<0.05, one-way ANOVA). **(B)** The total cumulative plasma S100B concentrations were estimated with area under the curve (AUC±SD). Statistical significance is indicated with alphabetical letters (n=8, p<0.05, one-way ANOVA).

Figure 4. Double immunostaining of occludin-1 and von-Willebrand factor. (A) The 3-D immuno-micrographs show the cerebral abundance of occludin-1 (shown in yellow) and von-Willebrand factor (vWF, shown in magenta) in the brains of the mice maintained on control low-fat chow, diet enriched in cholesterol or saturated fat (SFA) for 3 months. The dimensions of the micrographs are 138 μm (X axis), 98 μm (Y axis), and 12.5 μm (Z axis). **(B)** The total expression of cerebrovascular endothelium was quantitatively measured by estimating the voxel intensity of the fluorescent staining of von-Willebrand factor (vWF). The abundance of cerebrovascular occludin-1 was measured in the area where vWF and occludin-1 are colocalized, and express as relative to the vWF expression. Data are shown as mean±SEM. Statistical significance was indicated with alphabetical letters (n=8, p<0.05, one-way ANOVA).

Figure 5. Colocalization of cerebral IgG extravasation and astrocyte activation. The immunofluorescent images show the double immunolabelling of cerebral IgG and GFAP in the

cortex. Cerebrovasculature with significant cerebral IgG leakage induced by aging in 12 months low-fat fed mice were accompanied with substantial GFAP activation (red) whereas vessels with no IgG extravasation in 3 months low-fat fed mice showed no surrounding activated GFAP. The nuclei were counterstained with DAPI (blue). The images were taken at a magnification of x200 and the 3-D dimensions were 430 μm (X axis), 322 μm (Y axis) and 15 μm (Z axis).

Figure 6. 3-D semi-quantitative analysis of cerebral astrocyte activation. The activation of astrocytes in the cortex was semi-quantitatively analysed in mice maintained a low-fat diet, or a diet enriched in saturated fat diet (SFA) or cholesterol. **(A)** Voxel intensity of immunostained GFAP was measured per volume unit and express as mean±SEM. Data significantly differ from control (Dietary effects) are indicated by * (n=8, $p<0.05$, one-way ANOVA), and significance within each group (Aging/Duration effects) is indicated by alphabetical letters (n=8, $p<0.05$, one-way ANOVA). **(B)** The total cumulative activation index of astrocyte during the entire dietary intervention period was also estimated with area under the curve (AUC±SD). Statistical significance is indicated with alphabetical letters (n=8, $p<0.05$, one-way ANOVA). **(C)** Pearson's correlation between the cerebral IgG extravasation and GFAP expression was analysed.

Figure 7. Plasma lipid analysis. (A) The concentration of plasma total cholesterol and triglyceride were determined colorimetric assays in control low-fat fed mice and animals maintained on diets enriched in saturated fat (SFA) or choelsterol. **(B)** The correlation of plasma lipids versus blood-brain barrier dysfunction (IgG extravasation) was determined. **(C)** The data are shown as mean±SEM. Data significantly differ from control (Dietary effects) are indicated by * (n=8, $p<0.05$, one-way ANOVA), and significance within each group (Aging/Duration effects) is indicated by alphabetical letters (n=8, $p<0.05$, one-way ANOVA).

Table 1.

	Control	Cholesterol	SFA
Total Fat	4%	5%	20.3%
% total digestible energy from lipids	n/a	n/a	40%
Cholesterol	not detected	1.00%	not detected
SFA C12:0 and less	n/a	n/a	n/a
Myristic Acid 14:0	trace	trace	0.05%
Pentadecanoic Acid 15:0	n/a	n/a	0.01%
Palmitic Acid 16:0	0.20%	0.20%	5.16%
Magaric Acid 17:0	n/a	n/a	0.05%
Stearic Acid 18:0	0.10%	0.10%	7.31%
Arachidic Acid 20:0	n/a	n/a	0.24%
Behenic Acid 22:0	n/a	n/a	0.04%
Tetracosanoic Acid 24:0	n/a	n/a	0.03%
Palmitoleic Acid 16:1	trace	trace	0.05%
Heptadecenoic Acid 17:1	n/a	n/a	0.01%
Olecic Acid 18:1 n9	2.40%	2.40%	6.62%
Gadoleic Acid 20:1	trace	trace	0.01%
Linoleic Acid 18:2 n6	0.80%	0.80%	0.67%
Linoleic Acid 18:3 n3	n/a	n/a	0.05%
Linoleic Acid 18:3 n6	0.40%	0.40%	not detected
Stearidonic Acid 18:4 n3	n/a	n/a	n/a
Arachadonic Acid 20:4 n6	trace	trace	not detected
EPA 20:5 n3	trace	trace	not detected
DPA 22:5 n3	n/a	n/a	not detected
DHA 22:6 n3	trace	trace	not detected

Figure 1.

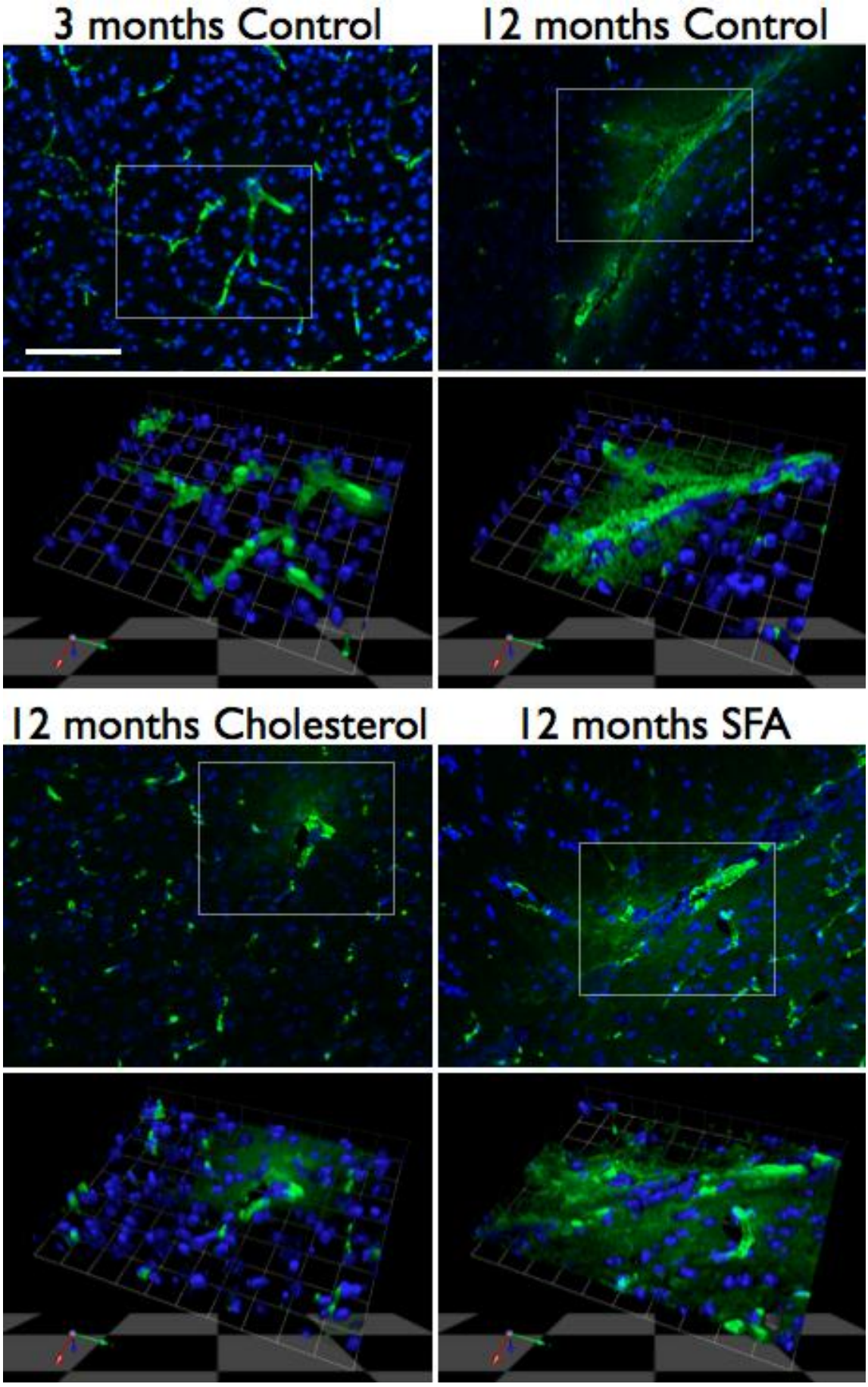
3 months Control
12 months Control
12 months Cholesterol
12 months SFA

Figure 2.

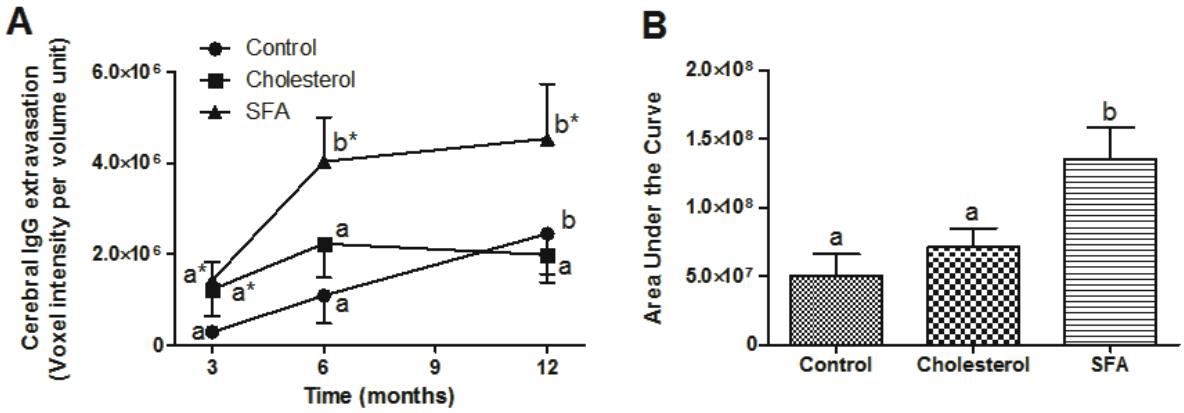
A
Cerebral IgG extravasation
(Voxel intensity per volume unit)
6.0×10⁶
4.0×10⁶
2.0×10⁶
0
Control
Cholesterol
SFA
b*
b*
a*
a*
a
a
b
a
a
3
6
9
12
Time (months)
B
Area Under the Curve
2.0×10⁸
1.5×10⁸
1.0×10⁸
5.0×10⁷
0
a
a
b
Control
Cholesterol
SFA

Figure 3.

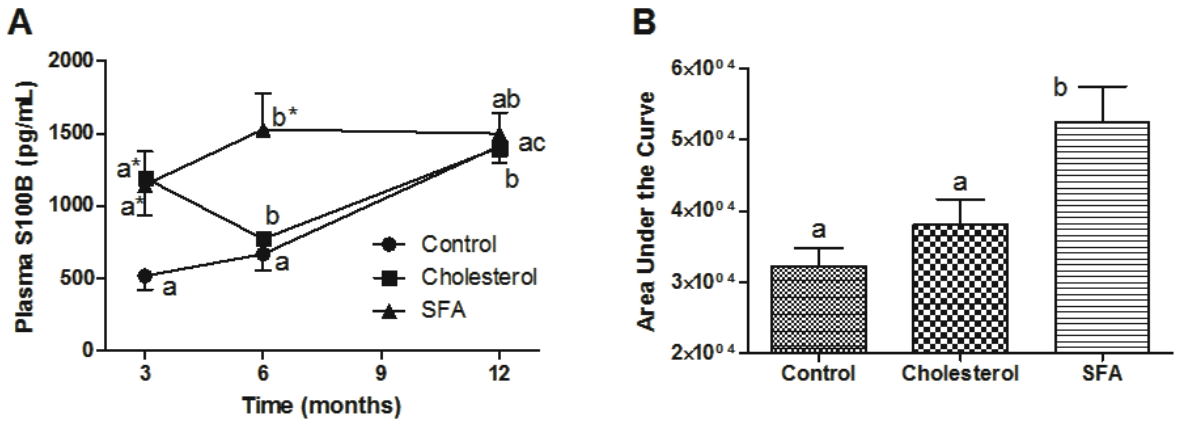
A
Plasma S100B (pg/mL)
2000
1500
1000
500
0
3
6
9
12
Time (months)
a*
a*
b*
ab
ac
b
b
a
a
Control
Cholesterol
SFA
B
Area Under the Curve
6x10^04
5x10^04
4x10^04
3x10^04
2x10^04
a
a
b
Control
Cholesterol
SFA

Figure 4.

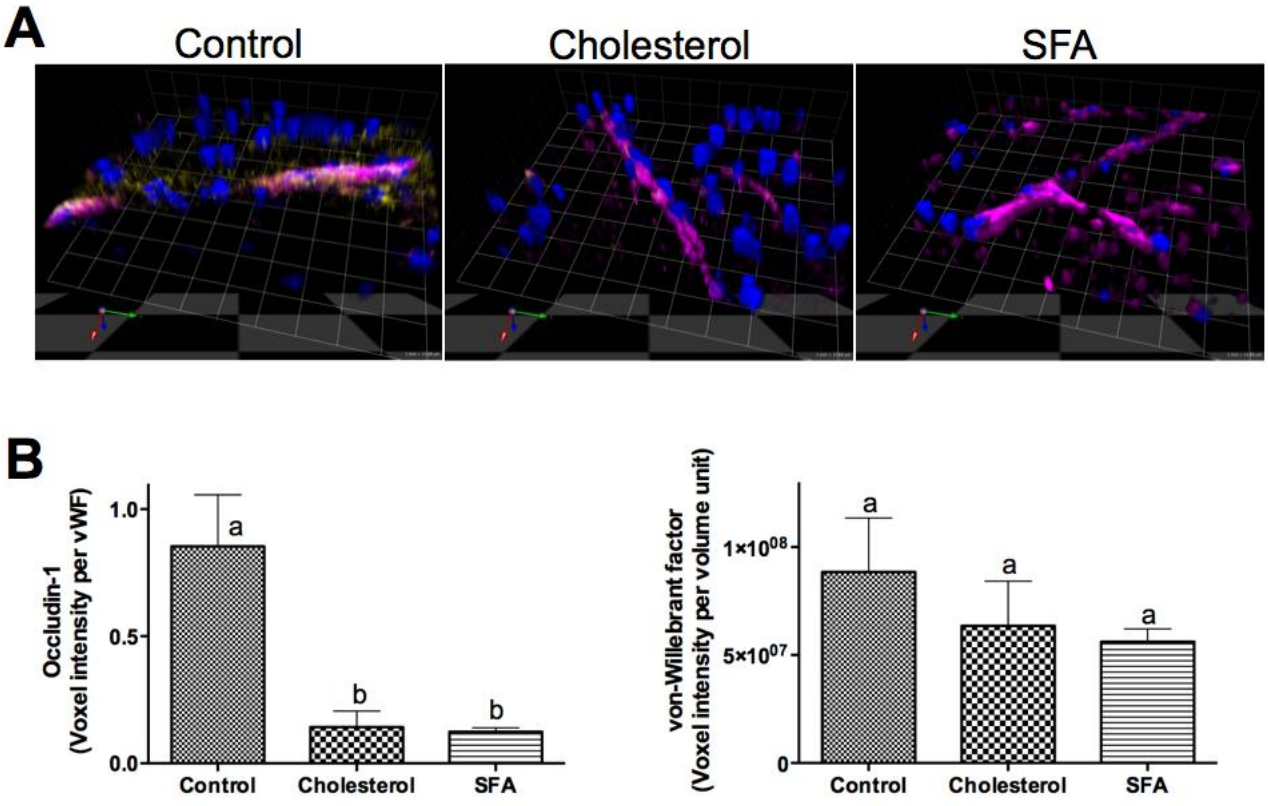
A
Control
Cholesterol
SFA
B
Occludin-1
(Voxel intensity per vWF)
1.0
0.5
0.0
a
b
b
Control
Cholesterol
SFA
von-Willebrant factor
(Voxel intensity per volume unit)
1×10^08
5×10^07
0
a
a
a
Control
Cholesterol
SFA

Figure 5.

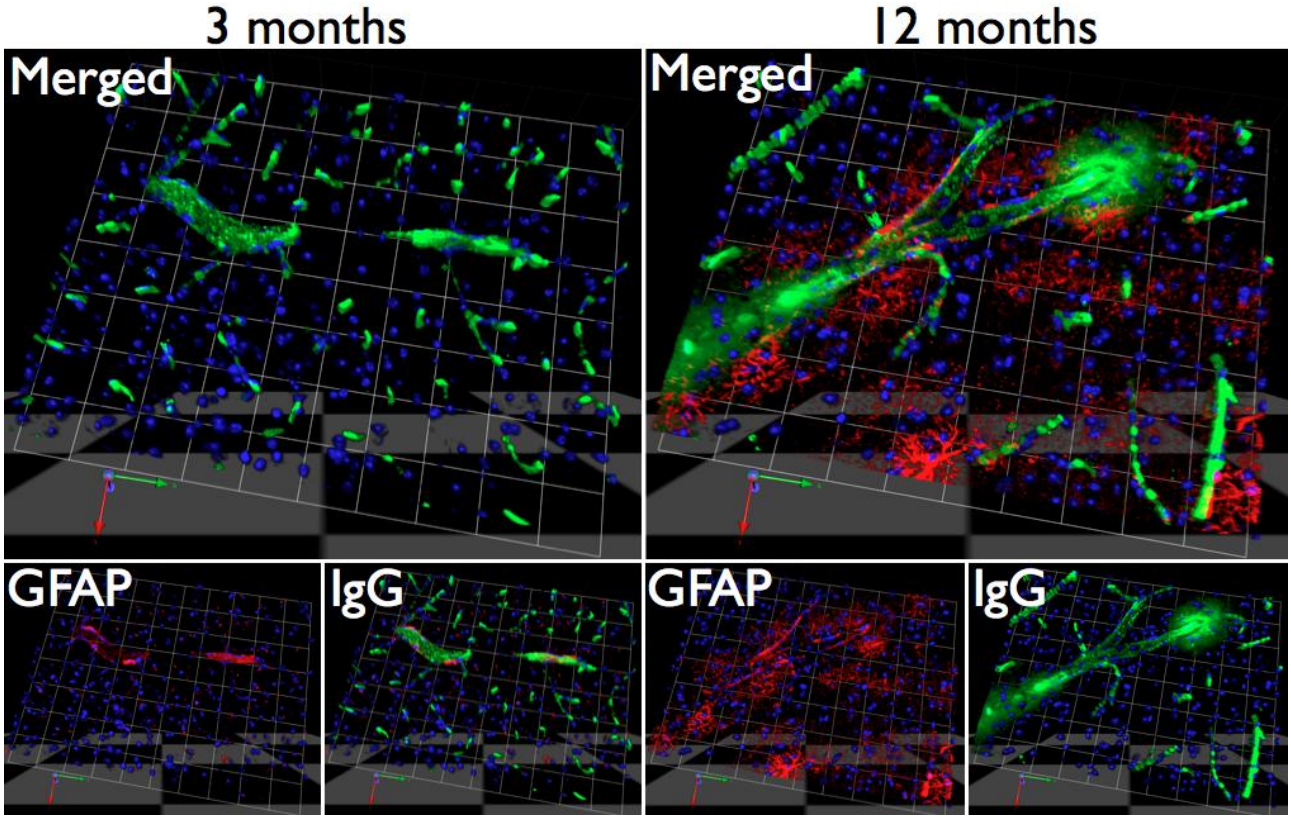

Figure 6.

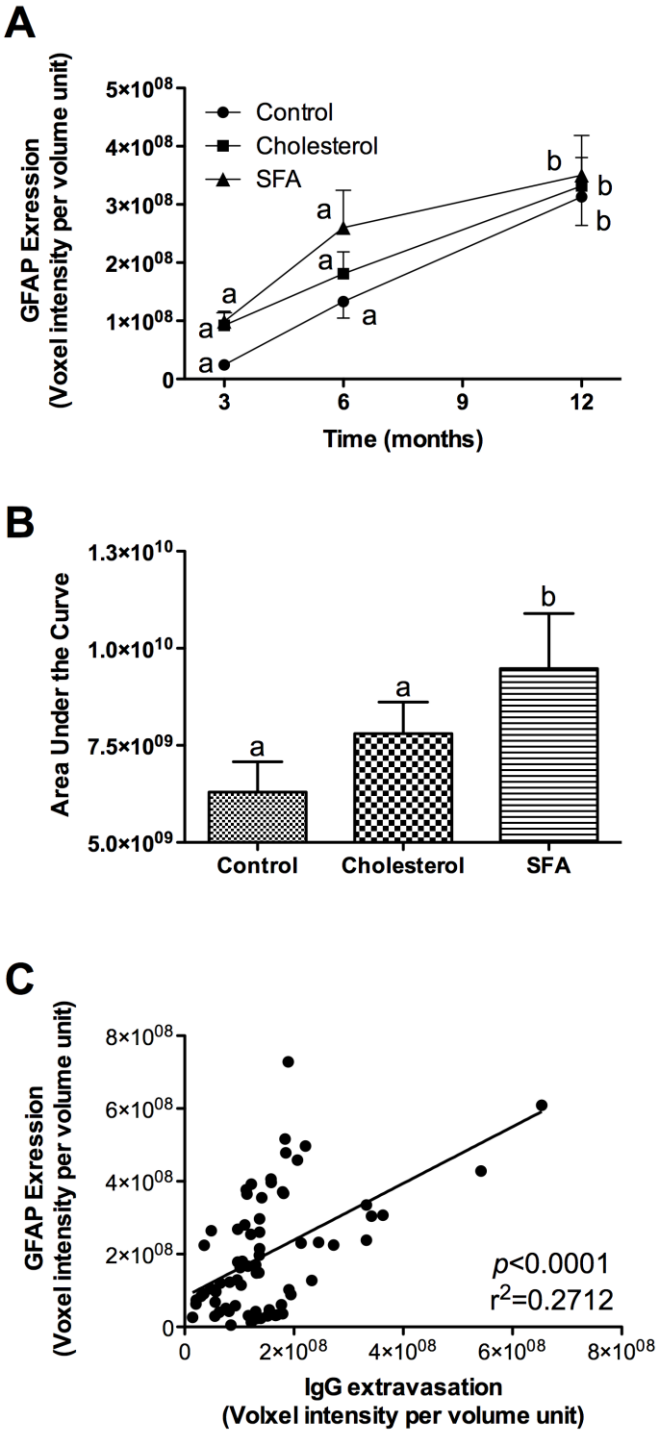
A
GFAP Exression (Voxel intensity per volume unit)
5×10^08
4×10^08
3×10^08
2×10^08
1×10^08
0
Control
Cholesterol
SFA
a
a
a
a
a
a
b
b
b
3
6
9
12
Time (months)
B
Area Under the Curve
1.3×10^10
1.0×10^10
7.5×10^09
5.0×10^09
a
a
b
Control
Cholesterol
SFA
C
GFAP Exression (Voxel intensity per volume unit)
8×10^08
6×10^08
4×10^08
2×10^08
0
p<0.0001
r^2=0.2712
0
2×10^08
4×10^08
6×10^08
8×10^08
IgG extravasation
(Volxel intensity per volume unit)

Figure 7.

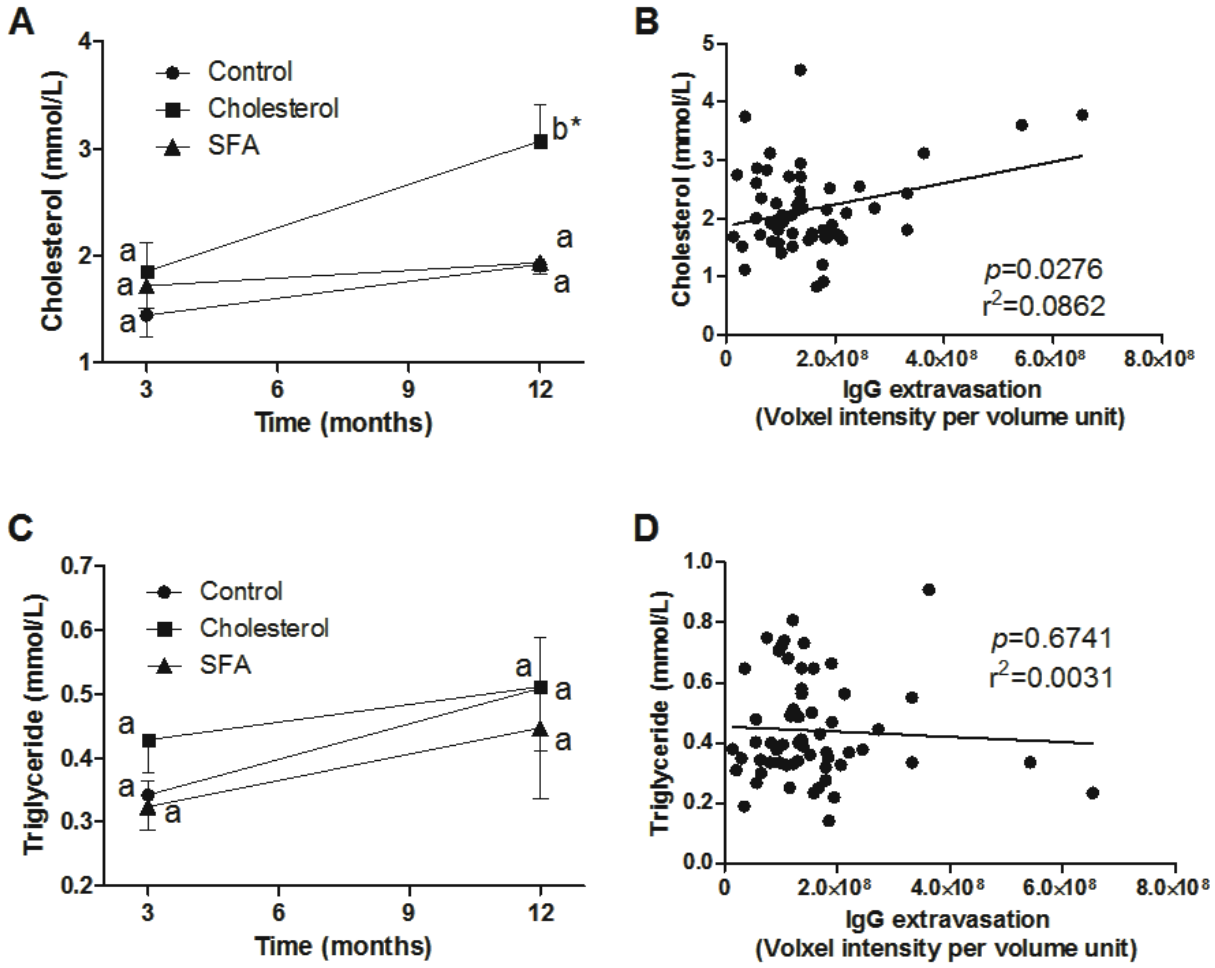
A
Control
Cholesterol
SFA
Cholesterol (mmol/L)
Time (months)
a
a
a
b*
a
a
B
Cholesterol (mmol/L)
p=0.0276
r2=0.0862
IgG extravasation
(Volxel intensity per volume unit)
C
Control
Cholesterol
SFA
Triglyceride (mmol/L)
Time (months)
D
Triglyceride (mmol/L)
p=0.6741
r2=0.0031
IgG extravasation
(Volxel intensity per volume unit)